Influence of processing parameters on the flow path in friction stir welding

J.A. Schneider[1], A.C. Nunes, Jr[2]

[1]Mechanical Engineering Department, Mississippi State University, Mississippi State, MS 39762

[2]NASA-Marshall Space Flight Center, Materials and Processes Laboratory, Metals Engineering Branch, EM30, Huntsville, AL 35812

Keywords: aluminum alloys, friction stir welding, FSW, metal flow path

Abstract

Friction stir welding (FSW) is a solid phase welding process that unites thermal and mechanical aspects to produce a high quality joint. The process variables are rpm, translational weld speed, and downward plunge force. The strain-temperature history of a metal element at each point on the cross-section of the weld is determined by the individual flow path taken by the particular filament of metal flowing around the tool as influenced by the process variables. The resulting properties of the weld are determined

by the strain-temperature history. Thus to control FSW properties, improved understanding of the processing parameters on the metal flow path is necessary.

Introduction

FSWing holds the promise of joining many alloys that are traditionally difficult to fusion weld, and has the potential to be useful for many applications. However, since this process was invented at the Welding Institute in 1991 [1], the mechanisms of this process are still being debated. At present, a trial and error approach is used to obtain a good weld, but this process is costly and it slows down the development time for the implementation of FSW into the production schedule. The process parameters could be predicted with a greater accuracy if the material flow pattern during FSW as a function of the pin tool geometry and process parameters were understood. To be able to prescribe the FSW process parameters from first principles, a better understanding of the physics of the material flow is required.

Most of what is known about the deformation flow path is deduced from the asymmetric flow patterns inferred from tracer studies. Initial tracer studies used preferential etching to study the mixing of dissimilar alloys [2, 3]. Definition of the flow paths in the FSW process was first obtained in a study by Colligan [4], in which the faying surface of the weld joint was embedded with 0.38mm diameter steel balls placed at various linear positions through the weld thickness and to either side of the weld tool. Post weld positioning of the steel balls, as investigated by x-ray radiography, suggested an orderly flow of the metal around the pin tool. Based on the entrance into the weld zone, only

some of the metal flow appeared to be forced downward by the threaded pin, while the rest appeared to be simply rotated from the front to the back of the pin tool [4].

Subsequent studies have looked at inserted copper foil, plated surfaces, and composite markers to further investigate these observations [5-7]. All studies indicated that the flow was orderly with the weld metal appearing to flow along defined paths or streamlines. Variations were observed in individual streamlines dependent on insertion location, vertically between shoulder and pin bottom and laterally between advancing side (AS) retreating side (RS). Based on the experimental studies, two models have been published which describe the metal flow as influenced by the processing parameters and weld tool geometry [8-10].

The 1st model uses a kinematic approach toward modeling of the metal flow path [8, 9]. Figure 1 illustrates how three incompressible component flow fields, established by the pin tool geometry, can be superimposed to construct a plausible model of the overall incompressible FSW flow field. The first component results from the rotation of the tool spindle and consists of a rigid body rotation, or rotating plug, which is bounded by a cylindrical shear surface. The second component results from the translation of the pin tool along the weld seam and adds a uniform velocity component to the rigid body rotation. The third component is induced by certain pin tool features (e.g. threads) and creates a ring vortex circulation component around the pin tool.

These 3 flow field components when combined produce two intertwined flow streams in the metal. Metal entering the FSW on the RS, engulfed and abandoned by the overall flow field around the tool during a brief fraction of rotation, is hardly influenced by the ring vortex flow component and simply flows through with little or no deviation from its insertion line. Metal entering on the AS is subjected to action by the ring vortex flow component for an appreciably longer segment of its path. The radial inward component of the ring vortex flow, generally encountered close to the tool shoulder, may trap the streamline within the flow field around the tool. Such a streamline spirals toward the bottom of the pin tool, where the radial component of the ring vortex flow reverses and allows the streamline to emerge from the tool flow field along a line deviating substantially, both laterally and vertically, from its insertion line. At each vertical level, from shoulder to pin bottom in classical FSW or shoulder to shoulder in self-reacting FSW, there is a critical point of insertion between AS and RS bounding a current of trapped, spiraling streamlines on the AS side and a current of streamlines undergoing no more than a full revolution around the tool on the RS. The intermingling of these two currents in the wake of the weld determines the major features of the weld macrostructure.

The 2nd model treats the FSW process in terms of metal working [10]. The process considers the movement of weld metal through 5 zones as illustrated in Figure 2. The rotating pin tool generates heat which softens the metal in advance of the FSW tool travel. The rotating motion of the weld tool forms the initial deformation zone in the softened metal which pushes the metal up toward the shoulder and down into an

extrusion zone. Once the metal enters the extrusion zone, it is moved around the rotating pin tool to exit in the wake. The FSW shoulder passes over the metal exiting the extrusion zone and forges it to ensure consolidation.

The objective of this study was to investigate the metal flow streamlines in a FSW under a variety of processing parameters using a 0.025mm diameter tungsten wire as a tracer. Post weld position of the tracer wire was examined using x-ray radiography. Although aspects of the metal working model [10] address the heat generation in FSWing, the resulting flow streamlines, as documented by the tracer wire in this study, appear to match the flow described by the kinematic model [8, 9].

Experimental

Rolled panels, 610mm (24") long and 6.35mm (0.25") thick, of aluminum alloy 2219-T87 was used in this study. A tungsten wire, 0.025mm (0.001") in diameter was positioned in a 0.025mm (0.001") deep groove scored along one side of the longitudinal seam side of the panel as illustrated in Figure 3. After positioning the wire, the plates are clamped together and tack welded to maintain the wire position. X-ray radiographs are used to ensure wire placement prior to clamping in the FSW fixture.

The panels were welded with the pin tool offset either to the AS or RS of the panel joint containing the wire or directly on the center of the panel joint. The weld tool consisted of a 12.7mm (1/2") -20 UNF LH threaded pin tool with a scrolled shoulder 30.5mm (1.2")

in diameter and a pin length slightly less than the plate thickness. All welds were terminated with a sudden stop (e-stop) of travel and rotation. Subsequently the embedded pin tool was unscrewed to remove it from the weld panel.

To establish nominal conditions for the AA2219 weld panels, a number of iterative trials were done to establish processing conditions producing adequate weld quality as evidenced by tensile tests. Off nominal conditions were then selected. Weld parameters are summarized in Table 1 for the 2219 panels. The effect of varied plunge force was studied in Series A. "Hot" or "cold" weld variations were studied in Series B and C. A "hot" weld is one with a higher rpm or slower travel speed. A "cold" weld is one with a lower rpm or higher travel speed.

Each nominally 610mm (24") long weld panel was subjected to a systematic variation of travel speed, rpm, or plunge force while maintaining the other two parameters constant. A 25.4mm (1") transition region separated each parameter change, resulting in a 165mm (6.5") weld length to characterize each parameter. Tracer positions were recorded using standard x-ray radiography equipment. Where noted, the x-ray radiographs have been inverted, such that higher density material appears darker, and marker wire positions traced to enhance the contrast.

Table I: Variation of Weld Parameters for 2219 Weld Panels

Series	Pin Tool Rotation (rpm)	Pin Tool Travel Speed, mm/s (ipm)	Downward Plunge Force, kN (lbs)
A	200	1.9 (4.5)	29, 31, 36 (6500, 7000, 8000)
B	150, 200, 300	1.9 (4.5)	31 (7000)
C	200	1.3, 1.9, 2.5 (3, 4.5, 6)	31 (7000)

Results and Discussion

The top or plan view of the FSW zone is illustrated in Figure 4. The flow zone around the pin tool is referred to as the rotating metal plug, and is separated from the parent material by a thin shear zone. Figure 4 illustrates the tracer wire entering the shear zone which bounds the rotating plug of metal. As a segment of tracer wire crosses the shear zone, the segment is pulled in tension by the rotating metal plug trying to rotate the wire while the base of the segment embedded in the parent material outside the shear zone holds it back. When the segment in the rotating plug is long enough for the shear force on its surface to separate it from the rest of the wire, the segment is captured by the plug, rotated, and abandoned to the wake of the weld. A sketch of a side view of the marker wire in the vicinity of the rotating metal plug is shown in Figure 5.

Figures 6-8 presents x-ray radiographs documenting the post-weld tracer wire placement for 3 weld panels. Each panel was subjected to a systematic variation of one weld parameter while the other two were held constant. This produced 3 weld segments approximately 165mm (6.5") in length per panel. The e-stop occurs in the final segment and is evident by the pin tool removal or exit hole. The tracer wire position is shown from the last 76mm (3") prior to a parameter change. Each figure shows an inverted x-ray radiograph of the plan view with a regular x-ray radiograph of the corresponding side view. For these 3 weld panels, the wire was introduced at the center of the plate thickness (3.3mm from the shoulder). Figures 6-8 show the weld portions at two places along the weld panel including the end of weld which contains the pin exit hole. The weld panels selected reflect the variations observed in the resulting flow path as the wire position entering the weld zone was varied and the effect of the variation of the processing parameters and are discussed in context with the kinematic model illustrated in Figure 1.

For the weld panel in Figure 6, the wire was introduced at 6.1mm (0.24") RS offset (just within the 6.4mm pin radius) from the centerline of the weld. The plunge load as varied while the tool rotation and tool travel velocity were held constant. The inverted x-ray radiograph in Figure 6a, shows the post-weld wire position to be displaced outward, exiting slightly toward the RS. A small outward radial velocity component (a ring vortex component) tending to expel a metal element a bit early from the rotating plug could account for such a displacement. The displacement of the tracer was unaffected by

plunge load over the range examined. This can be seen by comparison of Figure 6a (36 kN plunge load) and 6b (29 kN plunge load), where the wire segments in the weld wake line up in a linear fashion. Very little through-thickness tracer wire displacement was observed in the side view of the pin tool exit hole in Figure 6c.

For the weld panel in Figure 7, the wire position was changed and the same weld parameters were applied from the previous weld (Figure 6). The tracer wire was introduced at 3.1mm (0.12") RS offset (well within the 6.4mm pin radius) from the weld centerline. The inverted x-ray radiograph in Figure 7a shows the marker wire exiting along the same flow streamline as it entered the weld zone. In this weld panel, each band of weld metal in the wake contains one wire segment. Very little upward displacement was observed in the side view shown in Figure 7c, similar to the side view in Figure 6c. No effect of plunge loading on the post-weld tracer wire displacement was observed over the range of plunge loadings investigated as can be seen by comparison of Figure 7a (36 kN plunge load) and 7b (29 kN plunge load).

For the weld panel in Figure 8, the wire was introduced at 3.1mm (0.12") RS offset from the weld centerline, just as for the previous panel of Figure 7. However, for this weld panel, the tool rotation speed was varied while the plunge load and tool travel were held constant. The rpm was increased from 200 rpm (Figure 7) to 300 rpm for Figure 8a and decreased to 150 for Figure 8b. The increase from 200 rpm to 300 rpm produced an overall lateral tracer shift of about a pin radius towards the AS. Decreasing the tool

rotation from 300 rpm to 150 rpm restored the displacement to about what it was at 200 rpm.

The shift to the AS may result from a longer retention of the marker elements in the rotational field due to imposition of a radially inward velocity component, a result of an alteration of the ring vortex flow component. The ring vortex flow is a large slow temperature-sensitive circulation taking the form of a ring vortex encircling the pin-tool. The circulation is driven by threads on the pin and/or scrolls on the shoulder. The wire being placed at mid-depth on the pin, the radial component of the ring vortex is driven inward above the wire and outward below the wire. The radial component is expected to be small at the wire level and could be either inward or outward. A hotter weld (higher rpm) reduces the flow stress in the weld metal. Appreciable heat is generated at the shoulder that should raise the temperature in the upper (shoulder) regions around the pin. If the temperature field changes bring the upper part of the ring vortex field with its inward radial velocity component, down (away from the shoulder) the pin, this could explain the observed displacement toward the AS.

A noticeable amount of upward displacement is evident in the normal x-ray radiograph in Figure 8c of the exit hole side view. The outer part of the ring vortex flow component sweeps metal upward; the inner part, downward. The overall vertical marker displacement due to this flow component is complex enough so that it is more reliable to model it and make a computation. With hotter welds, however, it is anticipated that the

ring vortex flow effects should be enhanced. Enhanced ring vortex flow appears a good candidate for a cause of the enhanced vertical displacement with rpm.

In the panel of Figure 9 the tracer wire has been moved from the plate center closer to the shoulder, about 20% of the plate thickness 1.27mm (0.05") down from the shoulder. The rotating metal plug has a larger diameter as it approaches the shoulder as illustrated in Figure 5, about 20% larger in the present case judging from the radius at which the inserted wire begins to bend into the rotating flow field. Unlike Figures 6-8, the inverted x-ray radiograph shown in Figure 9a shows an apparently random scattering of tracer wire segments.

The normal x-ray radiograph of the side view of the exit hole in Figure 9c, shows the tracer wire being drawn up toward the shoulder at the top of the pin and then pushed downward, finally exiting in the wake close to the bottom of the pin. This tracer wire shows evidence of a longer entrapment in the rotating plug. The material closest to the shoulder tends to be trapped most deeply in the down-spiraling flow inside the rotating plug and tends to emerge farthest down the pin. (If weld metal that crosses the shear zone boundary of the rotating plug is recrystallized, and if the metal entering the rotating plug at the upper part of the pin is translated to the lower part of the pin, the recrystallized part of the FSW should be on the lower part of the pin.

A magnified view of the weld seam, shown in Figure 10, as it approaches close to the tool shows an increasing seam deflection up to a shear on the order of several hundred

percent, followed by a sudden incorporation of the seam into a sharply defined boundary between parent metal and a fine recrystallized metal structure next to the tool. The shear zone has width and structure. It can be imagined as composed of concentric ring elements each rotating with its own angular velocity ω. The angular velocities increase from zero at the outer edge to the angular velocity of the tool at the inner edge, assuming no slippage at the tool interface. At radius r the shear rate $\dot{\gamma}$ is, given a continuous variation of rotation ω(r) in equation 1,

$$\dot{\gamma} = r\frac{d\omega}{dr} \qquad (1)$$

If the angular velocity drops from ω of the rotating plug to zero over distance δ, $\dot{\gamma} \approx \frac{\omega r}{\delta}$.

If the time to cross the boundary is $\frac{\delta}{V}$ at the centerline, the shear increment is $\frac{\omega r}{V}$, where V is the weld speed [9]. The strain increment would be on the order of 10,500% for weld panel C20 (Figure 8). The actual strain rate is not known until the width of the transformation interface δ is known, but it must be high, on the order of shear rates encountered in metal cutting.

Conclusion

The wire tracer approach of mapping of the weld metal flow streams can be used as a basis for establishing the metal flow paths as a function of FSW parameters, although it may still prove difficult to get information on FSW flow very close to the pin. Of the three parameters studied, weld speed plunge force and tool rotational speed, rotational

speed was found to have the most influence on the displacement of tracer metal. A number of complex tracer observations all seem explicable using concepts of a sharply defined shear zone enveloping the FSW pin-tool, and three flow components: a rotating plug flow, a translational flow, and a ring vortex flow as described by the kinematic model.

Acknowledgements

Funding was provided by NASA-Marshall Space Flight Center Cooperative Agreement #NNM04AA14A. The authors wish to thank Mr. Sam Clark and Mr. Ronnie Renfroe at the NASA-MSFC for working together to produce the welds and Mr. John Ratliff at the NASA-MSFC for shooting the x-ray radiographs.

References

1) W. M. Thomas, et. al., "Friction stir butt welding," Int'l Patent Appl. No. PCT/GB92102203 and Great Britain Patent Appl. No. 9125978.8.

2) Y. Li, L.E. Murr, J.C. McClure, Solid-State Flow Visualization in the Friction Stir Welding of 2024 Al to 6061 Al, *Scripta Mater.*, 40/9 (1999) p. 1041-1046.

3) L.E. Murr, Y. Li, R.D. Flores, E.A. Trillo, J.C. McClure, Intercalation vortices and related microstructural features in the friction-stir welding of dissimilar metals, *Mat. Res. Innovat.*, 2 (1998) p. 150-163.

4) K. Colligan, Material Flow Behavior during Friction Stir Welding of aluminum, *Welding Research Supplement*, (1999) p. 229s-237s.

5) T.U. Seidel, A.P. Reynolds, Visualization of the Material Flow in AA2195 Friction-Stir Welds using a Marker Insert Technique, *Met. & Mat. Trans. A*, 32A (2001) p. 2879-2884.

6) M. Guerra, C. Schmidt, J.C. McClure, L.E. Murr, A.C. Nunes, Jr., Flow patterns during friction stir welding, *Mat'ls Characterization*, 49 (2003) p. 95-101.

7) B. London, M. Mahoney, W. Bingel, M. Calabrese, R.H. Bossi, D. Waldron, Material flow in friction stir welding monitored with Al-SiC and Al-W composite markers, *Proc. Symp. on FSW & Processing II*, TMS (Warrendale, PA.), ed. K.W. Jata, M.W. Mahoney, R.S. Mishra, S.L. Semiatin, T. Lienert, (2003) p. 3-12.

8) J.A. Schneider and A.C. Nunes Jr., Characterization of Plastic Flow and Resulting Microtextures in a Friction Stir Weld, *Met. Trans. B* (2004) 777-783.

9) A.C. Nunes, Jr., Wiping Metal Transfer in Friction Stir Welding, *Aluminum 2001: Proc. 2001 TMS Annual Mtg Automotive Alloys & Joining Aluminum Symp.*, TMS Pub., ed. G. Kaufman, J. Green, S. Das, (2001) p. 235-248.

10) W.J. Arbegast, Modeling Friction Stir Joining as a Metal Working Process, *Hot Deformation of Aluminum Alloys*, TMS publisher, ed. Z. Jin (2003).

List of Figures

6. Weld panel C02A with weld parameters of 200 rpm, 1.9mm/s (4.5 ipm) and varying load. Tracer wire is introduced to the weld nugget at 6.1mm (0.24") offset to the RS and at a depth of 3.3mm (0.13"). a) inverted x-ray radiograph of the weld termination showing pin tool exit hole with plunge load of 36 kN (8000 lbs), b) inverted x-ray radiograph of the section of plan view at 29 kN (6500 lbs) plunge load, and c) normal x-ray radiograph of the side view of the pin tool exit hole at 36kN (8000 lbf).

7. Weld panel C05 with weld parameters of 200 rpm, 1.9mm/s (4.5 ipm) and varying load. Tracer wire is introduced to the weld nugget at 3.1mm (0.12") offset to the RS and at a depth of 3.3mm (0.13"). a) inverted x-ray radiograph of the weld termination showing pin tool exit hole with plunge load of 36 kN (8000 lbs), b) inverted x-ray radiograph of the section of plan view at 29 kN (6500 lbs) plunge load, and c) normal x-ray radiograph of the side view of the pin tool exit hole at 36 kN (8000 lbs).

8. Weld panel C20 with weld parameters of 31kN (7000 lbs), 1.9mm/s (4.5 ipm) and varying tool rotation. Tracer wire is introduced to the weld nugget at 3.1mm (0.12") offset to the RS and at a depth of 3.3mm (0.13"). a) inverted x-ray radiograph of the weld termination showing pin tool exit hole with tool rotation of 300 rpm, b) inverted x-

ray radiograph of the section of plan view at 150 rpm tool rotation, and c) normal x-ray radiograph of the side view of the pin tool exit hole at 300 rpm.

9. Weld panel C22 with weld parameters of 31kN (7000 lbs), 1.9mm/s (4.5 ipm) and varying tool rotation. Tracer wire is introduced to the weld nugget at the panel center line and at a depth of 1.27mm (0.05"). A) inverted x-ray radiograph of the weld termination showing pin tool exit hole with tool rotation of 300 rpm, b) inverted x-ray radiograph of the section of plan view at 150 rpm tool rotation, and c) normal x-ray radiograph of the side view of the pin tool exit hole at 300 rpm.

10. Weld seam ahead of pin tool for weld panel C05. Note severity of deformation prior to incorporation into plug.

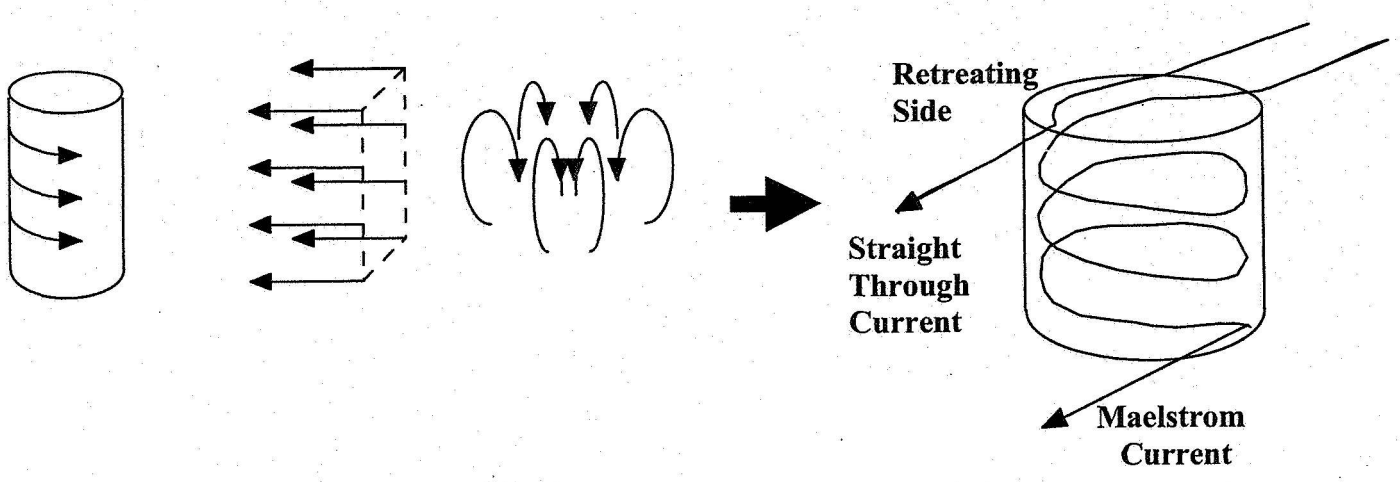

(a) (b) (c) (d)

Figure 1.

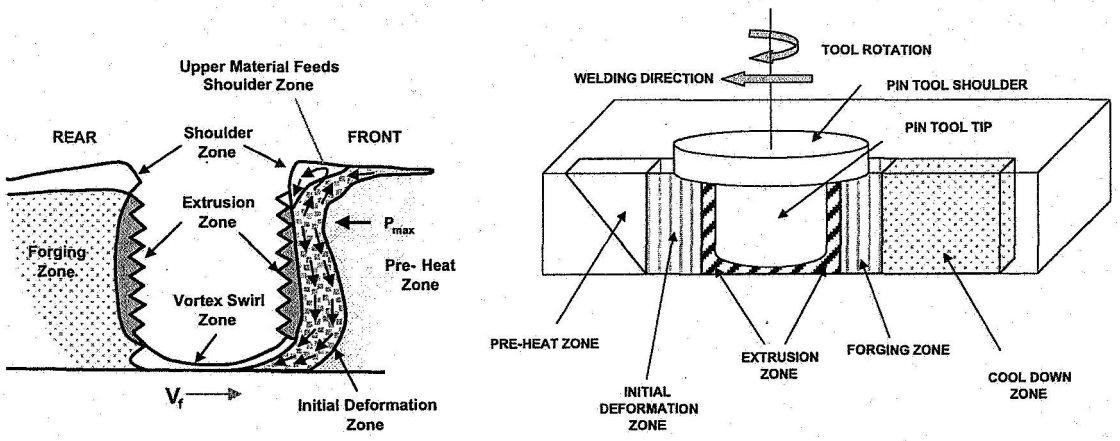
Upper Material Feeds
Shoulder Zone
REAR
Shoulder
Zone
FRONT
Extrusion
Zone
P_{max}
Forging
Zone
Pre- Heat
Zone
Vortex Swirl
Zone
V_f
Initial Deformation
Zone
TOOL ROTATION
WELDING DIRECTION
PIN TOOL SHOULDER
PIN TOOL TIP
PRE-HEAT ZONE
INITIAL
DEFORMATION
ZONE
EXTRUSION
ZONE
FORGING ZONE
COOL DOWN
ZONE

Figure 2.

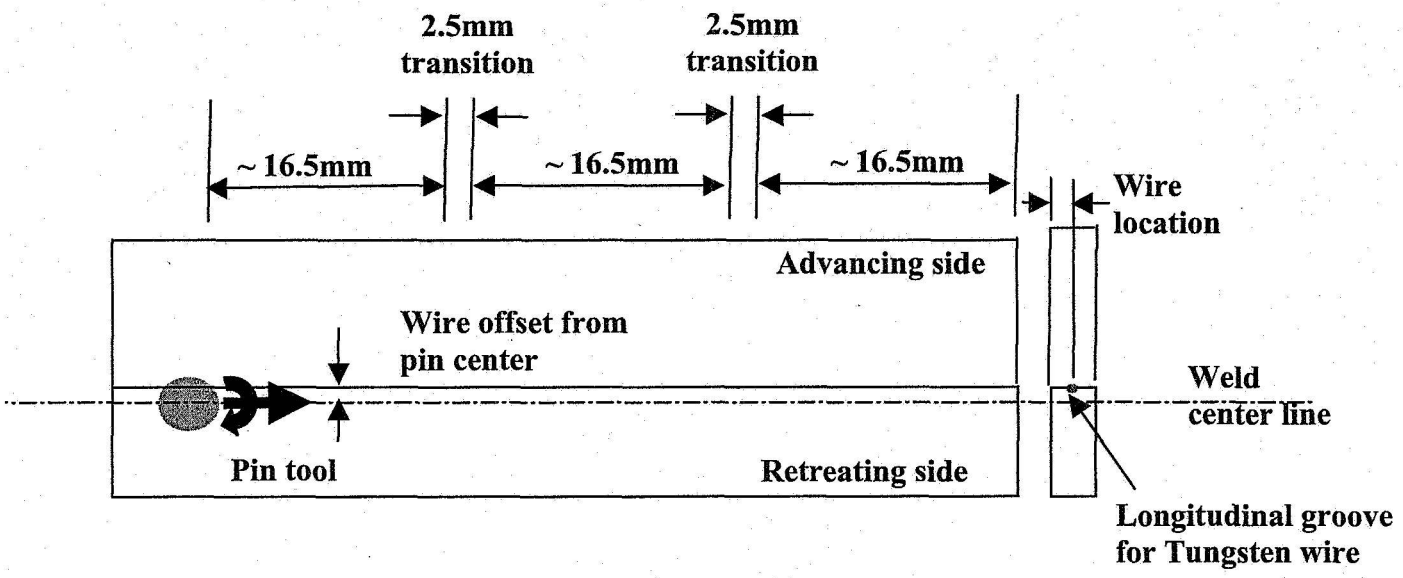
2.5mm
transition
2.5mm
transition
~ 16.5mm
~ 16.5mm
~ 16.5mm
Wire
location
Advancing side
Wire offset from
pin center
Weld
center line
Pin tool
Retreating side
Longitudinal groove
for Tungsten wire

Figure 3.

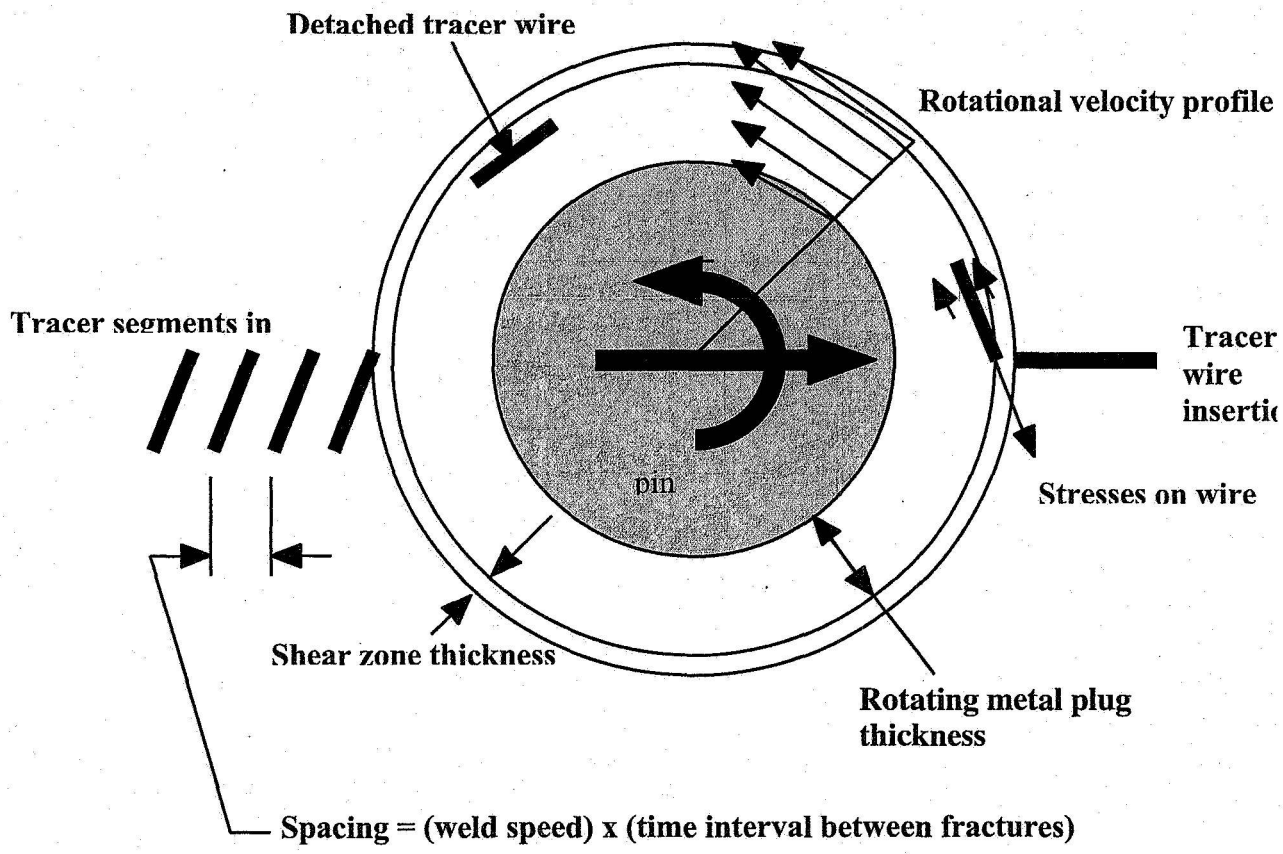
Detached tracer wire
Rotational velocity profile
Tracer segments in
Tracer
wire
insertic
pin
Stresses on wire
Shear zone thickness
Rotating metal plug
thickness
Spacing = (weld speed) x (time interval between fractures)

Figure 4.

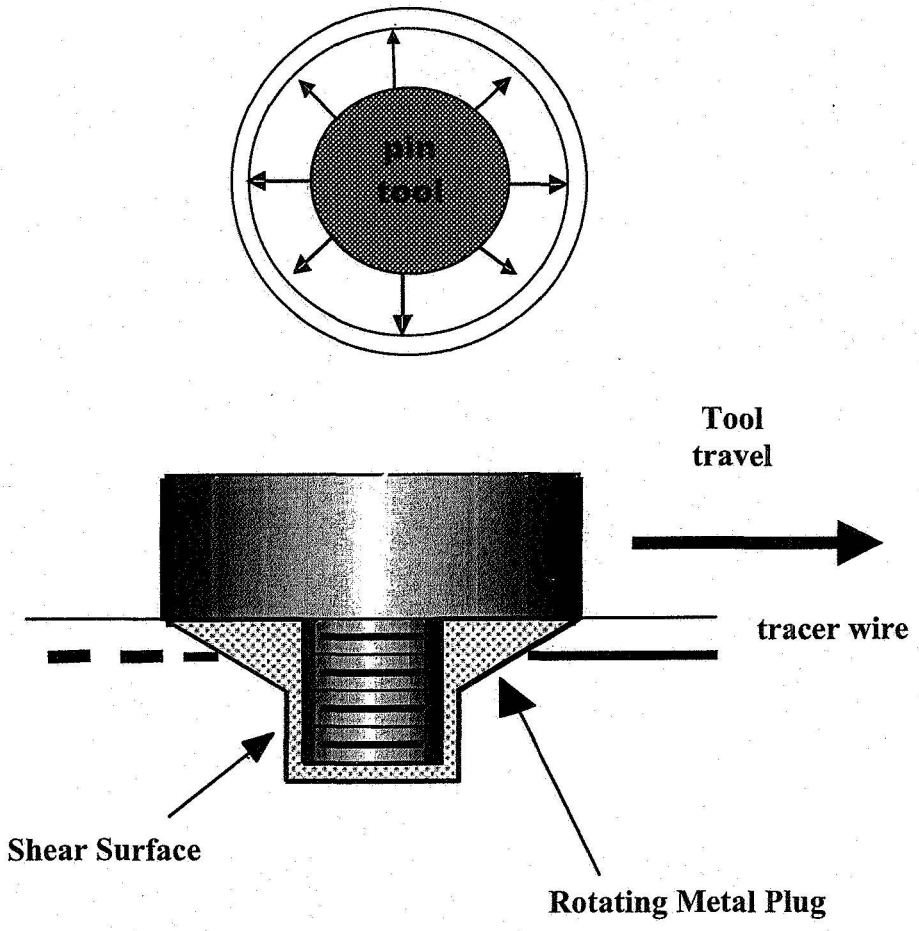
pin
tool
Tool
travel
tracer wire
Shear Surface
Rotating Metal Plug

Figure 5.

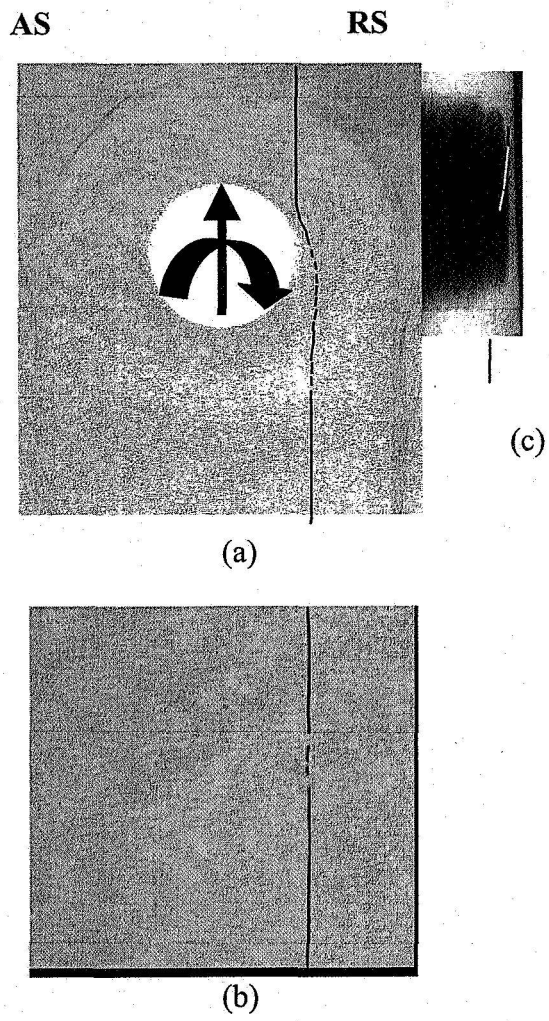

Figure 6.

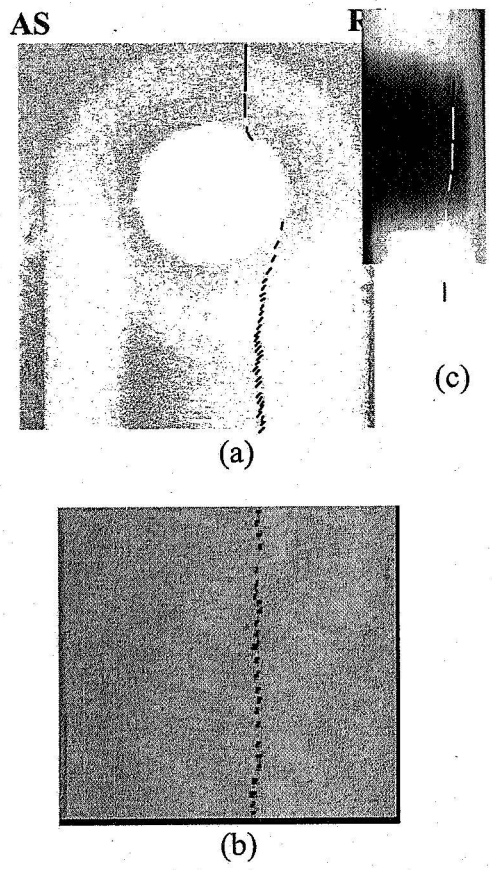

Figure 7.

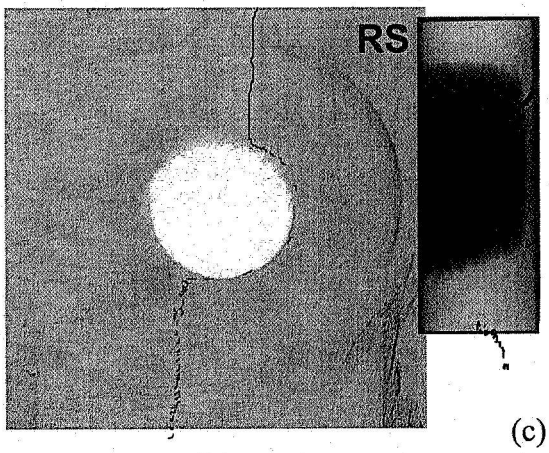

(a)

(c)

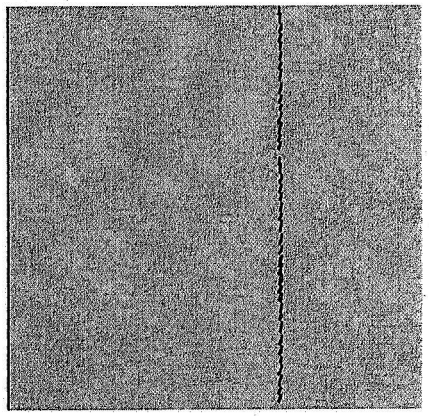

(b)

Figure 8.

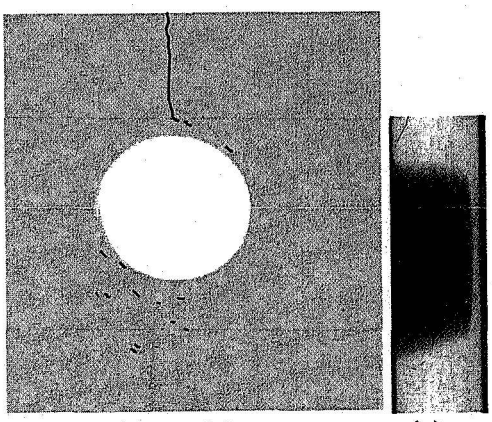

(a) (c)

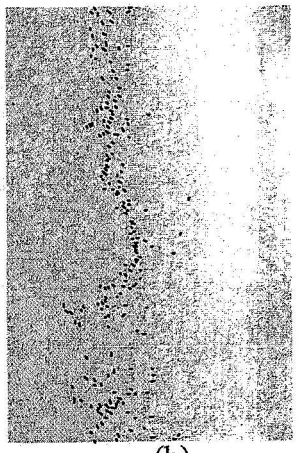

(b)

Figure 9.

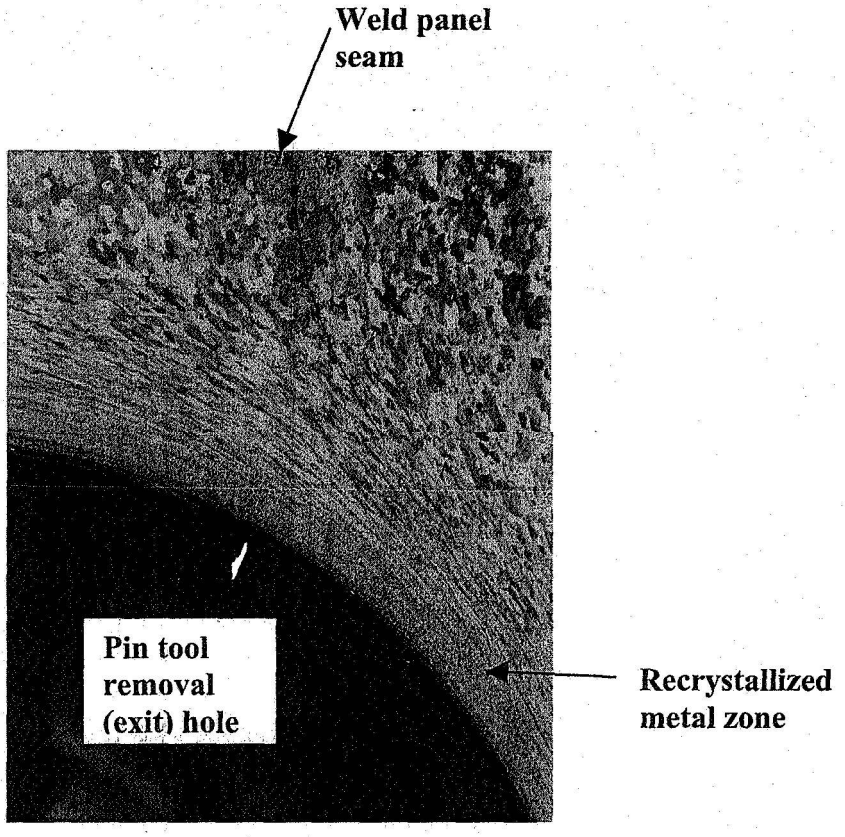
Weld panel seam
Pin tool removal (exit) hole
Recrystallized metal zone

Figure 10.